ELSEVIER

Physica C 274 (1997) 165-172

PHYSICA C

Linear response in the AC susceptibility of vortices in $YBa_2Cu_3O_7$ crystals with columnar defects

G. Pasquini [a,*], P. Levy [a], L. Civale [b], G. Nieva [b,1], H. Lanza [a]

[a] Departamento de Física, CNEA, Av. del Libertador 8250, 1429, Buenos Aires, Argentina
[b] Centro Atómico Bariloche, CNEA, 8400 Bariloche, Argentina

Received 30 May 1996; revised manuscript received 4 September 1996

Abstract

We explore the AC magnetic susceptibility of $YBa_2Cu_3O_7$ single crystals with columnar defects. For vortices parallel to the defects the linear response is mainly determined by the Campbell penetration depth with a field independent Labusch parameter indicating that vortices are individually pinned. The small dissipation in this limit is likely to arise from thermal fluctuations of vortex segments between pairs of metastable states (two-level systems) in the Bose glass phase. Tilting vortices away from the tracks results in a reduction of the Bose glass temperature and an increase of the dissipation due to the reduction of the pinning forces. We discuss the onset of nonlinear response as the AC field increases.

Keywords: Columnar defects; AC susceptibility; Campbell penetration

1. Introduction

Aligned columnar defects introduced by heavy-ion irradiation strongly influence vortex dynamics in high-temperature superconductors (HTSC's) [1,2]. The geometry of these defects is very well suited to pin vortex lines, and it is now well established that large enhancement of the critical currents and substantial enlargement of the irreversible regime can be achieved [1]. Below a melting temperature T_{BG} and for applied fields parallel to the defects, vortex matter freezes into a Bose glass phase [2-6] with zero linear resistivity. Theoretical models [2,3] indicate that at low temperatures and for applied fields much smaller than the matching field B_Φ (the field at which vortex and defect densities are the same), inter-vortex interactions are weak as compared to vortex-defect interactions, thus each vortex is localized inside a single track and pinning is strong. As field increases and vortices become closer together, inter-vortex interactions become important and pinning turns collective. The line in the H-T phase diagram that traces the smooth crossover between individual and collective pinning has been called the "accommodation field", $B^*(T)$. As T increases and approaches a temperature T^*, the "entropic effect" drastically reduces the effective pinning energy and B^* decreases sharply. The situation for $T > T^*$ is complex and less understood. The perpendicular component of the vortex localization length grows with T and at a temperature $T_1 > T^*$ it equals the average defect distance. Above T_1 each vortex is collectively pinned by several defects. The combination of the dose-independent characteristic temperature T^*,

* Corresponding author. Fax: +54 1 754 7121; e-mail: pasquini@tandar.cnea.edu.ar.

[1] Member of the CONICET, Argentina.

PII S0921-4534(96)00528-X

a defect-density dependent characteristic temperature T_l and a field-dependent inter-vortex interaction determines a variety of possible pinning regimes.

Measurements of the AC susceptibility χ have been extensively used [7] to explore the vortex dynamics of HTSC at high temperatures (in the vicinity of the "irreversibility line"), in systems with both correlated [4,8,9] and non-correlated disorder [10,11]. The interpretation of these measurements is not simple. Vortex motion in the various solid and liquid phases is influenced by pinning, thermal fluctuations and viscosity [12–15]. The AC response may be either linear or nonlinear [16], and critical scaling may be observed in the vicinity of the vortex-glass [10] or Bose glass [6] transition. Recent theoretical studies indicate that the AC response of systems with aligned columnar defects should exhibit a variety of linear and nonlinear regimes depending on the value and orientation of the applied DC field H_{DC}, the temperature T and the amplitude h_{AC} and frequency f of the AC field [17]. An additional complication arises from the geometry. The solution of the electromagnetic problem of an AC field applied perpendicular to the surface of a thin platelet (which is the typical case for HTSC crystals and thin films), is non-trivial. Only recently have the quantitative correlation between the macroscopic experimental results $\chi(H_{DC}, h_{AC}, f, T)$ and the underlying vortex motion been sorted out in full, and only for the two extreme limits of linear response [18] and critical state [19].

In this work we present measurements of the AC susceptibility χ of $YBa_2Cu_3O_7$ single crystals with columnar defects introduced by heavy-ion irradiation, in the limit of low magnetic fields and high temperatures. Our results are consistent with existing models [9,12,13,15] for the motion of vortices in the presence of pinning. For small values of h_{AC} we find a linear response that is well described by a Campbell regime [20] of pinned vortices. In this limit we observe a very small and almost frequency-independent dissipation that is likely to originate in thermally induced jumps of vortex segments between two metastable states of similar energy (two-level systems) [14] in the Bose glass phase. Quantitative results for the Campbell penetration depth and the Labusch parameter that characterize this regime are obtained using the numerical procedure recently developed by Brandt [18]. For larger h_{AC} the amplitude of vortex oscillations grow and the response becomes nonlinear when the linear approximation for either the pinning or thermal forces fails. The crossover from linear to nonlinear response thus provides information about the size of the pinning centers.

2. Experimental details

Several $YBa_2Cu_3O_7$ single crystals grown using a flux growth technique [21] were irradiated at room temperature with 280 MeV Sb^{22+} ions at the TANDAR accelerator facility, in a variety of doses and orientations. Energy deposition rate is greater than the threshold for columnar track formation ($\sim$ 1.8 keV/Å) in the first 10 μm. Measurements of DC magnetization confirm a large enhancement of the critical currents, enlargement of the irreversible regime and alignment effects, as shown by previous studies [1,4]. To perform the AC measurements the crystals were fixed to one coil of a compensated secondary pair rigidly built up inside a long primary coil that can rotate with respect to the DC field H_{DC}. This setup ensures an AC field parallel to the c-axis being highly homogeneous, and a low noise level that allows us to vary the AC field from 5 mOe to 6 Oe. Here we will report on results for a crystal of size 1 mm × 1 mm × 8 μm, irradiated at an angle of 15° off the c-axis to a dose equivalent to a matching field B_Φ = 3000 G. This low defect density results in a very small decrease (15 mK) in the as-grown T_c = 92 K, and no detectable broadening of the transition.

3. Response for h_{AC} parallel to the columnar defects

Fig. 1 shows curves of the screening and dissipative components of the AC susceptibility, $\chi'(T)$ and $\chi''(T)$ for a DC field H_{DC} = 730 Oe parallel to the columnar defects. All the curves are normalized to the total step in χ' measured with the same AC field and frequency at zero DC field. Measurements were performed at a frequency f = 91 kHz, and each curve corresponds to a different value of h_{AC}. These data differ in several respects from those measured on the same crystal before irradiation. The step in $\chi'(T)$ and the peak in $\chi''(T)$ shift to higher temperature and become

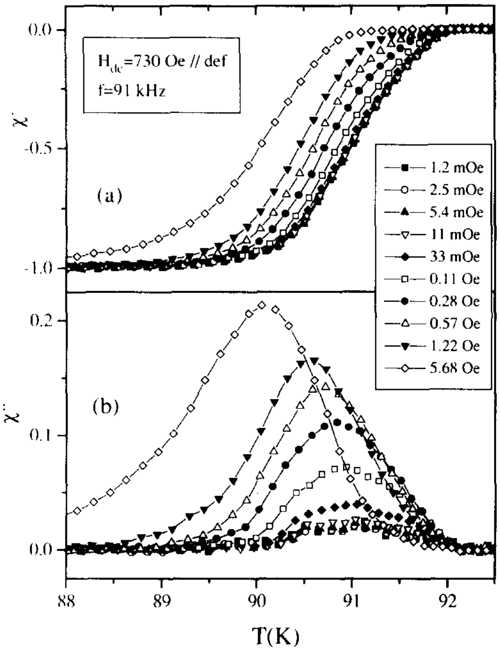

Fig. 1. Temperature dependence of the (a) out-of-phase χ' and (b) in-phase χ'' components of the AC susceptibility, for a DC field H_{DC} parallel to the defects and various AC fields h_{AC}. For low h_{AC} a linear regime with a small dissipation peak is observed.

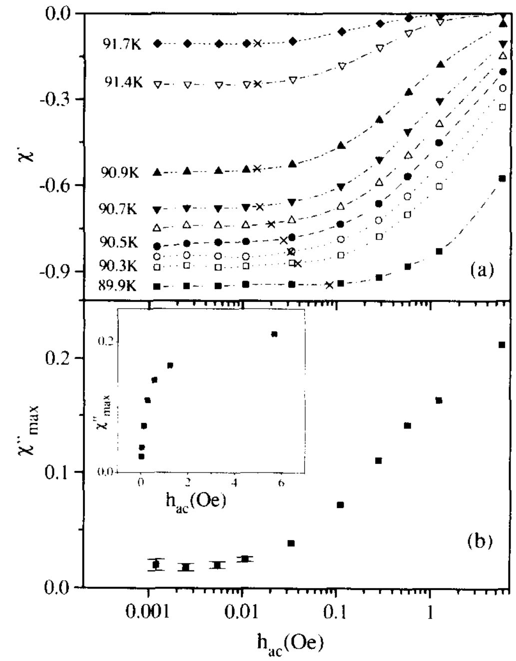

Fig. 2. (a) Out-of-phase component χ' of the AC susceptibility for various temperatures and (b) maximum height of the in-phase component χ'', as a function of AC field h_{AC}. The crosses in (a) indicate the onset of nonlinear response. The inset shows the same data as in (b), in a linear scale.

much sharper, consistent with the enhanced pinning and expansion of the irreversible regime [1,4,9]. Before irradiation, the transition width increased strongly with both H_{DC} and h_{AC}. After irradiation, in contrast, the transition shows no significant broadening as either H_{DC} or h_{AC} grow. Finally, the peak in $\chi''(T)$ for the same h_{AC} is much smaller after irradiation.

We see in Fig. 1 that the response is nonlinear, i.e., χ' and χ'' depend on h_{AC}. To explore this behavior in more detail, in Fig. 2 we have used the data in Fig. 1 to construct curves of χ' versus h_{AC} (Fig. 2(a)), and the height of the peak χ''_{max} versus h_{AC} (Fig. 2(b)). We observe that the response is amplitude independent for low h_{AC} and becomes amplitude dependent (i.e. non-linear) as h_{AC} grows. Data for other fields $H_{DC} \leq 730$ Oe are very similar. This behavior is a fingerprint of vortex pinning. When the h_{AC} superimposed to H_{DC} is small enough, vortices perform harmonic elastic oscillations within their pins and the response is linear [8,20]. A peculiarity of the observed linear regime at low h_{AC} is the very small height of the dissipation peak, $\chi''_{max} \simeq 0.02$, indicating that vortex motion is almost non-dissipative in that limit. When h_{AC} increases vortex excursions become larger and the response turns nonlinear. For large enough h_{AC} vortices are driven out of their pinning sites and a critical state develops. Calculations for the critical state in the transverse disk geometry predict [19] $\chi''_{max} \simeq 0.24$. Consistently, for our largest $h_{AC} = 5.7$ Oe we observe $\chi''_{max} \simeq 0.22$ and a trend to saturation, as seen in the inset of Fig. 2 (we will approximate our crystal geometry with a disk of radius 0.7 mm).

In contrast to the above scenario, vortex motion in the absence of pinning is well described by an ohmic flux-flow regime [12,13,15], characterized by a linear response for all h_{AC} and a large dissipation peak, $\chi''_{max} \simeq 0.44$ for the transverse disk geometry [18], in clear disagreement with the behavior seen in Figs. 1 and 2.

4. Angular dependence

To confirm the importance of the columnar character of the defects we have explored the AC response

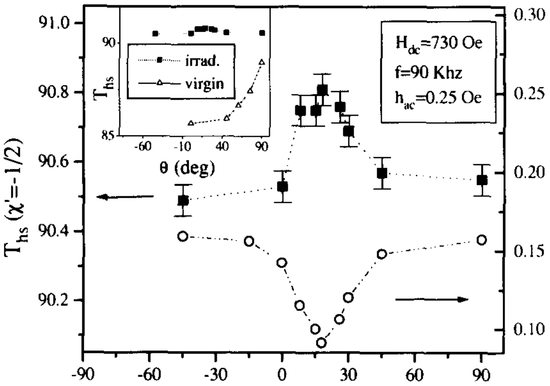

Fig. 3. Angular dependence of the maximum in the χ'' peak and the temperature of half screening (T_{hs}) in the irradiated sample. The inset shows the comparison with $T_{hs}(\theta)$ before irradiation.

for different orientations of H_{DC}. In Fig. 3 we plot the temperature T_{hs} at which half screening occurs, (i.e., $\chi'(T_{hs}) = -\frac{1}{2}$), as a function of the angle θ between H_{DC} and the crystallographic c-axis. We observe that T_{hs} maximizes when H_{DC} is parallel to the tracks within our experimental error. This behavior proves that vortex pinning arises from the columnar defects, and is consistent with the expectation that the Bose glass transition temperature is largest when $B \parallel$ tracks [2]. The comparison of $T_{hs}(\theta)$ before and after irradiation (shown in the inset) indicates that the intrinsic anisotropy of the crystal is completely superseded by the effect of the columnar defects. As an additional evidence of the influence of the vortex-track alignment, in Fig. 3 we have plotted the angular dependence of the maximum of the dissipation χ''_{max}. We find that χ''_{max} is lowest for H_{DC} parallel to the tracks, indicating that the ratio of pinning forces to dissipative forces is largest for such configuration.

5. Linear response

We now concentrate on the linear regime of the $H_{DC} \parallel$ tracks configuration. The linear AC response is determined [12,13,15,18] by the penetration depth $\lambda_{AC}(T, B, \omega)$, where $\omega = 2\pi f$. If no dissipative mechanisms were involved in the vortex motion equation λ_{AC} would be real and $\chi'' = 0$. Dissipative processes give rise to a complex valued $\lambda_{AC} = \lambda_R + i\lambda_I$ and $\chi'' \neq 0$. The function $\chi(\lambda_{AC})$ depends on the sam-

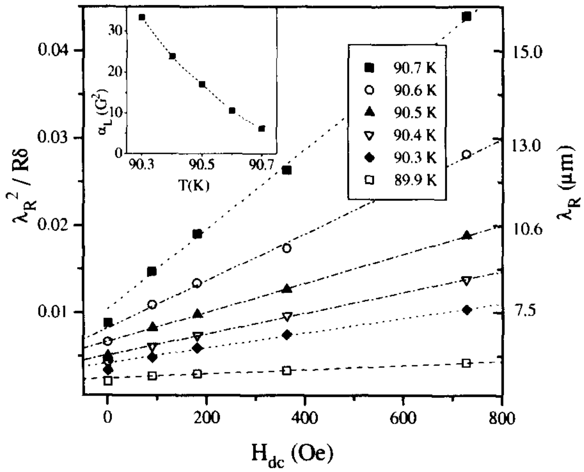

Fig. 4. Square of the real penetration depth λ_R normalized by the characteristic length $(R\delta)^{1/2}$ as a function of DC field H_{DC}, obtained from $\chi'(\lambda_R)$ in the linear regime. The straight lines are least squares fits used to determine the field-independent Labusch parameter α_L (see text). The inset shows the temperature dependence of α_L.

ple geometry. Brandt [18] showed that for a disk of radius R and thickness δ in a transverse AC field $\chi + 1 \approx \sum_n^N [c_n / (\Lambda_n + \varphi)]$, where $\varphi = R\delta / 2\pi\lambda_{AC}^2$ and the constants Λ_n and c_n are real. The sum arises from the discretization involved in the numerical procedure, and an accurate approximation can already be obtained [18] with $N = 20$.

When $\lambda_I / \lambda_R = \varepsilon \ll 1$, to first order in ε we obtain

$$\chi' + i\chi'' \approx -1 + \sum_{n=1}^{N} \frac{c_n}{\Lambda_n + \varphi_R} + i\left[2\varphi_R \sum_{n=1}^{N} \frac{c_n}{(\Lambda_n + \varphi_R)^2} \right] \varepsilon, \qquad (1)$$

where $\varphi_R = R\delta / 2\pi\lambda_R^2$ is real. If we call $g(\varphi_R)$ the expression between brackets in Eq. (1), numerical evaluation shows that $0 \le g(\varphi_R) \le 0.46$, thus $\chi'' = g(\varphi_R)\varepsilon \ll 1$ as we observe. In this approximation χ' depends only on φ_R and Eq. (1) can be numerically inverted to obtain $\lambda_R(\chi')$. The result of this procedure is shown in Fig. 4, where $\lambda_R^2/R\delta$ is plotted as a function of H_{DC} for various T. The approximate values of λ_R are shown in the right axis. In all cases a small enough h_{AC} was used to ensure a linear response.

In the $\varepsilon \ll 1$ limit we expect $\lambda_R^2(T, B) =$

$\lambda_L^2(T) + \lambda_C^2(T,B)$, where $\lambda_L(T)$ and $\lambda_C(T,B) = (B\Phi_0/4\pi\alpha_L)^{1/2}$ are the London and Campbell penetration depths, respectively [12,13]. The Labusch parameter α_L measures the restoring force of the pinning well [20] taken as parabolic for small vortex displacements. We find that $\lambda_C^2 \propto H_{DC} \approx B$ as shown by the straight lines in Fig. 4, indicating that our data are well described by a Campbell regime [8,20] with a field-independent α_L. The temperature dependence of $\alpha_L(T)$ is shown in the inset. This is one of the main results of this work. A field-independent α_L strongly suggests that vortices are individually pinned. Indeed, when vortices are collectively pinned the effective pinning potential is related to the volume of the bundles and thus α_L depends on vortex density [12,13,15].

It is useful to analyze this result within the framework of existing models for pinning by columnar defects. For $T \to 0$ the theory predicts that the accommodation field $B^*(T) \sim B_\Phi$ [2,3]. As T increases and approaches a characteristic defect-density independent "depinning temperature" T^*, the "entropic effect" drastically reduces the effective pinning energy and B^* decreases sharply. Both theoretical expectations have been recently confirmed experimentally in $YBa_2Cu_3O_7$ single crystals irradiated with 1 GeV Au ions [5]. The depinning temperature was found to be rather low, $T^* \approx 40$ K, indicating that pinning efficiency is significantly less than unity (the theoretical estimate for optimum pinning gives $T^* \approx 0.8T_c$). Interestingly, we found an almost identical value of T^* for our crystals, which are irradiated with a much lower ion energy [22].

For $T > T^*$ pinned vortices start to wander away from their pinning centers. The transverse localization length, determined by the mean amplitude of the thermal fluctuations, grows exponentially [3] with T and becomes equal to the average distance between defects at a new characteristic temperature $T_l > T^*$. Above this defect-density dependent temperature each vortex is collectively pinned by several defects. Using the relations developed in Ref. [3] and the experimental result $T^* \approx 40$ K, we estimate $T_l \approx 85$ K. The large difference between T_l and T^* in our case is due to the long average distance between defects determined by the low irradiation dose. For $T^* < T < T_l$ the accommodation field $B^*(T)$ is predicted to exhibit an exponentially decreasing tail, crossing over to a $\sim T^{-6}$ dependence for $T > T_l$. Following the estimates of Blatter et al. [3] we find that the expectation for $B^*(T)$ in our temperature range is of the order of a few G, thus most of our data should be in the collective pinning regime. This appears to be in disagreement with our observation of a field-independent Labusch parameter up to fields above 700 Oe. We do not have an explanation for such discrepancy. We note, however, that no experimental determination of $B^*(T)$ in the high-temperature limit is available, and many aspects of the above theoretical expectations are still untested. A final comment on this respect is that the critical current density in the high temperature collective regime is predicted [3] to grow as $B^{1/4}$. If α_L follows the same behavior then the field dependence may be very small. Clearly, this issue requires further analysis.

If vortices are individually pinned, and considering that our data is in the regime $T > T_l$, then $\alpha_L(T)$ characterizes the elementary interaction between one vortex and several columnar defects in the limit of very large localization length. At these high temperatures the pinning potential is expected to be shallow due to the large influence of the thermal fluctuations, with an effective radius of the order of the superconducting coherence length $\xi_{ab}(T)$. If we consider, as an estimate [3], that the potential energy per unit length of a vortex segment at a distance R from the center of a track is $\varepsilon(R,T) = \varepsilon_r(T)/[R^2/2\xi^2 + 1]$, then the Labusch parameter $\alpha_L(T) = \varepsilon_r(T)/\xi^2(T)$ is a direct measure of the pinning energy per unit length $\varepsilon_r(T)$.

6. Dissipation in the linear regime

The presence of a linear response at low h_{AC} is expected based on general grounds both in liquid and glassy phases. Several different regimes can be distinguished depending on the relative importance of the various processes determining the vortex motion, as discussed by van der Beek in the case of non-correlated disorder [15]. Recent studies indicate that in the presence of correlated disorder the situation is qualitatively similar [17], but up to now these predictions have not been contrasted with the experiment. Dissipation processes introduce a phase shift between the driving force and the vortex motion, thus producing an imaginary part of λ_{AC} and a non-zero in-phase component χ''. The small χ'' observed in our measurements indicates that dissipative forces are much smaller than the

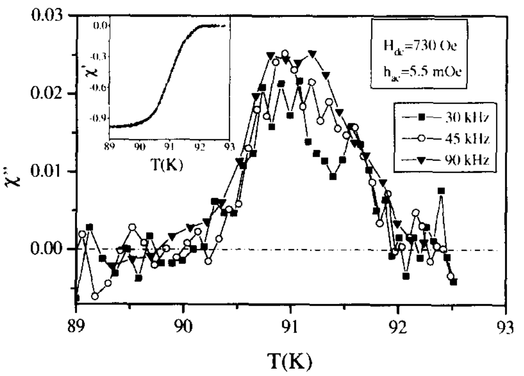

Fig. 5. Temperature dependence of the in-phase component χ'' in the linear regime for various frequencies. The inset shows the out-of-phase component $\chi'(T)$ at the same frequencies.

pinning force. Each dissipation mechanism produces a particular frequency dependence in λ_{AC}, that in the $\varepsilon \ll 1$ limit becomes manifest mainly in the frequency dependence of the in-phase component χ'' according to Eq. (1). Fig. 5 shows $\chi''(T)$ in the linear regime ($h_{\mathrm{AC}} = 5.5$ mOe) for $H_{\mathrm{DC}} = 730$ Oe and $f = 30$, 45, and 90 kHz. We are at the limit of our experimental resolution and equivalent data at lower f becomes unreliable due to the decreasing signal-to-noise ratio.

Two dissipative mechanisms related to vortex motion must be analyzed [12,15], namely viscous losses and thermal fluctuations (flux creep). If only the first one is considered, then λ_{AC} takes the form $\lambda_{\mathrm{AC}}^2 = \lambda_{\mathrm{L}}^2 + \lambda_{\mathrm{C}}^2(1 - \mathrm{i}\omega\tau_0)^{-1}$, where $\omega = 2\pi f$, the characteristic time $\tau_0 = \eta/\alpha_{\mathrm{L}}$ and η is the viscous drag coefficient. In the $\omega\tau_0 \ll 1$ limit, this gives $\lambda_I \simeq \frac{1}{2}(\lambda_{\mathrm{C}}^2/\lambda_R)\omega\tau_0$ with $\lambda_R = (\lambda_{\mathrm{L}}^2 + \lambda_{\mathrm{C}}^2)^{1/2}$, thus $\chi'' \simeq \frac{1}{2}(\lambda_{\mathrm{C}}/\lambda_R)^2 g(\varphi_R)(\omega\tau_0) \propto \omega$. In spite of the noisy character of data in Fig. 5, it is clear that χ'' is not proportional to ω, thus the viscosity is not the main contribution to dissipation. This is expected at our low frequencies. Indeed, from the experimental $\alpha_{\mathrm{L}}(T)$ and the Bardeen–Stephen result $\eta(T) \approx \Phi_0 H_{c2}/c^2\rho_{\mathrm{n}}$, where $\rho_{\mathrm{n}} \approx 2\times10^5$ Ω cm is the normal-state resistivity near the transition and $H_{c2} = (1.6\times10^4\ \mathrm{G/K})(T_c - T)$ is the upper critical field, we estimate $\tau_0(90.7\ \mathrm{K}) \approx 3\times10^{-8}$ s. Thus viscous losses can only account for a small fraction of the observed dissipation.

In contrast to viscosity, flux-creep dissipation has different frequency dependences in the liquid and glass phases. In the liquid phase activation barriers related to plastic distortions U_{pl} remain finite for $J \to 0$ and a linear resistivity arises from thermally assisted flux flow (TAFF). When this contribution dominates over viscous losses, $\lambda_{\mathrm{AC}}^2 = \lambda_{\mathrm{L}}^2 + \lambda_{\mathrm{C}}^2(1 + \mathrm{i}/\omega\tau)$, where $\tau \simeq \tau_0 \exp(U_{\mathrm{pl}}/kT)$. The result $\lambda_I \ll \lambda_R$ implies $\omega\tau \gg 1$, i.e. $U_{\mathrm{pl}} \gg kT$. Under these conditions we obtain $\lambda_I \simeq \frac{1}{2}(\lambda_{\mathrm{C}}^2/\lambda_R)/\omega\tau$, thus $\chi'' \simeq \frac{1}{2}(\lambda_{\mathrm{C}}/\lambda_R)^2 g(\varphi_R)/(\omega\tau) \propto \omega^{-1}$. Once again, it is clear from Fig. 5 that this behavior is not observed. We must still consider the combination of both mechanisms, that gives [12,13]

$$\lambda_{\mathrm{AC}}^2 = \lambda_{\mathrm{L}}^2 + \lambda_{\mathrm{C}}^2\left(-\mathrm{i}\omega\tau_0 + \frac{1}{1 + \mathrm{i}/\omega\tau}\right)^{-1}. \tag{2}$$

hen $\omega\tau_0 \ll 1$ and $\omega\tau \gg 1$ we get $\chi'' \simeq \frac{1}{2}g(\varphi_R)(\omega\tau_0 + 1/\omega\tau)(\lambda_{\mathrm{C}}/\lambda_R)^2$, thus TAFF ($\chi'' \propto 1/\omega$) and viscous losses ($\chi'' \propto \omega$) should dominate at low and high frequencies, respectively, and the minimum dissipation should occur at a frequency $\omega_0 = (\tau\tau_0)^{-1/2}$, where both contributions are equal. This possibility can also be ruled out. Indeed, even in the vicinity of ω_0 a three-fold variation in ω should produce a change in χ'' above our resolution. Moreover, τ_0 and particularly τ should exhibit a strong temperature dependence in the range of Fig. 5. As a result, the relative importance of both contributions, and thus the frequency dependence of χ'', should vary significantly with temperature, contrary to the experimental observation. We conclude that neither TAFF nor viscosity are the main sources of the observed dissipation.

We now analyze flux-creep dissipation in the Bose glass phase. Here activation barriers diverge for $J \to 0$ and TAFF is absent [2,3]. For finite current density J, pinned vortex configurations are characterized by a broad distribution of activation energies. Koshelev and Vinokur [14] proposed that for small J, when the jump rate is small, flux creep will influence the AC response primarily via jumps of vortex bundles between two nearby metastable states of similar energy. Although they focused on systems with non-correlated disorder, only the glassy character was taken into account in the analysis, thus an analogous mechanism should occur in systems with columnar defects. These "two-level systems" (TLS) give rise [14,15] to a linear response with average vortex displacement $\langle u\rangle \approx (\Phi_0/c)A_{\mathrm{tl}})J$, with

$$A_{\mathrm{tl}} = \frac{n_{\mathrm{tl}}}{4kT}\left\langle \frac{V^2r^2}{(1+\mathrm{i}\omega\tau_{\mathrm{tl}})\cosh^2(\Delta/kT)}\right\rangle, \tag{3}$$

where V, r, Δ and τ_{tl} are the volume, distance between states, energy difference between the two levels and characteristic jump time respectively, n_{tl} is the density of TLS and $\langle\cdots\rangle$ means average over the TLS. We can calculate the penetration depth in this regime,

$$\lambda_{\mathrm{AC}}^2 = \lambda_{\mathrm{L}}^2 + \lambda_{\mathrm{C}}^2(1+\alpha_{\mathrm{L}}A_{\mathrm{tl}}). \tag{4}$$

In the limit of small dissipation

$$\lambda_I \approx \tfrac{1}{2}(\lambda_{\mathrm{C}}^2/\lambda_R)\alpha_{\mathrm{L}}\,\mathrm{Im}\{A_{\mathrm{tl}}\}$$

and the main effect on χ'' will arise from TLS with $\Delta \le kT$ and $\omega\tau_{\mathrm{tl}} \approx 1$. Due to the broad distribution of τ_{tl} values, for any ω there will be approximately the same density of "tuned" TLS, then χ'' will be almost frequency independent [14,15], as we observe. In a Bose glass at low vortex density, TLS should primarily consist of vortex segments of length L jumping between nearby columnar defects via double-kink structures, thus $\mathrm{Im}\{A_{\mathrm{tl}}\} \approx (n_{\mathrm{tl}}^*/4kT)\langle L^2r^2\rangle \approx Ld_0^2/4kT$, where the last approximation assumes a linear density of active systems $n_{\mathrm{tl}}^* \approx 1/L$ and a separation between states of the order of the defect distance $d_0 \approx 800$ Å. Then $\chi'' \simeq \frac{1}{2}g(\varphi_R)(\lambda_{\mathrm{C}}/\lambda_R)^2\alpha_{\mathrm{L}}(Ld_0^2/4kT)$ and using the experimental values of χ'' and α_{L} we can estimate $L \approx 3500$ Å at 90.7 K. We conclude that a distribution of TLS in the Bose glass phase may account for the small and almost frequency-independent dissipation found in our studies.

In the Bose glass phase viscous losses are still present. By writing a combination analogous to Eq. (2) it can be seen that it should produce a contribution linear in ω, but the absence of ω dependence as well as the above numerical estimates indicate that viscous losses can be disregarded to first approximation. TLS also give a contribution to the real component of the AC penetration, that is hard to distinguish from λ_{C} due to the lack of ω dependence (see inset of Fig. 5). However, an estimate similar to the one above indicates that in our case $\alpha_{\mathrm{L}}\mathrm{Re}\{A_{\mathrm{tl}}\} \ll 1$ and the screening component is still nearly $\lambda_R = (\lambda_{\mathrm{L}}^2+\lambda_{\mathrm{C}}^2)^{1/2}$.

7. The onset of nonlinearity

To obtain additional information about the nature of the pinning centers, we analyze the onset of nonlinear response, clearly visible in Fig. 2 as a crossover from amplitude-independent to amplitude-dependent behavior as h_{AC} increases. As the dynamics is dominated by the restoring force of the pinning potential, the displacement of a vortex located at a distance ρ from the center of the sample, $u(\rho)$, is in phase with the local current density $j(\rho)$. The vortex motion equation takes the simple form

$$(1/c)\phi_0\, j(\rho) \approx \alpha_{\mathrm{L}}u(\rho). \tag{5}$$

This linear response breaks down when the displacement $u(\rho \approx R)$ of the vortices near the edge of the disk (those that perform the largest oscillations) exceeds a limiting value r_l. Following the numerical procedure described by Brandt [18] and using our experimental values of $\lambda_R(T, H_{\mathrm{DC}})$ (obtained from fits as those of Fig. 4), we calculate the sheet current $J(\rho)$ in the linear regime. We then obtain the real current density in the sample $j(\rho) = (c/4\pi)(h_{\mathrm{AC}}/R)\ J(\rho)$, which is proportional to h_{AC}. Using these results and Eq. (5) we can express the h_{AC} at which the nonlinearity first develops as

$$h_{\mathrm{AC}}^l(T, H_{\mathrm{DC}}) = \frac{4\pi\alpha_{\mathrm{L}}}{\phi_0}\frac{R}{J(R)}r_l, \tag{6}$$

where the only unknown is r_l. We can now compare this result with the experimental data. The crosses in Fig. 2 are the calculated values of $h_{\mathrm{AC}}^l(T)$ for H_{DC} = 730 Oe, using r_l = 25 Å as a fitting parameter. We see that the trend of $h_{\mathrm{AC}}^l(T)$ predicted by the very simple relation (6) coincides reasonably well with the experimental behavior.

The physical meaning of r_l is not obvious. A nonlinear response will develop as soon as the amplitude of vortex oscillations are large enough to invalidate either the harmonic approximation of the pinning potential or the linearity of the random thermal force. We note that r_l approximately coincides with the radius [1] of columnar defects (35–40 Å), and it is clearly smaller than the total effective radius $\sim \xi_{ab}(T)$ of the pinning potential ($\sim$ 130 Å at T = 90.7 K). One consequence of this fact is that the current density associated with the onset of nonlinear AC response is much smaller than the critical current density.

8. Conclusions

The AC susceptibility of $YBa_2Cu_3O_7$ crystals with columnar defects was studied, at low DC fields and high temperatures. We found a linear regime at low h_{AC} that can be satisfactorily described using existing models for the response of pinned vortices. The linear screening component χ' is dominated by a Campbell penetration depth with a frequency and field-independent Labusch parameter, suggesting that vortices are individually pinned even at these high temperatures. The Campbell regime extends to higher h_{AC} as T decreases (see Fig. 2), consistently with the expectation as the pinning energy increases. Dissipation in this regime is very small, indicating that vortex motion is mainly controlled by the pinning force produced by the columnar defects. As the applied field is tilted away from the tracks, the pinning energy decreases and the ratio of dissipative to pinning forces grows, thus producing an increase in χ'' as seen in Fig. 3. The identification of the origin of this small dissipation, associated to the motion of pinned vortices for current densities below the critical, has a significant technological interest as it determines the AC losses in high-T_c wires and tapes. Two-level systems appear to be the most likely source of dissipation, although measurements in a broader frequency range are clearly necessary to clarify this point.

Acknowledgements

We thank the technical staff of the TANDAR for their help during the irradiations. We thank G. Blatter for showing us his unpublished results, and L. Krusin-Elbaum, A. Koshelev, M. Goffman, F. de la Cruz, J. Guimpel and J.R. Clem for useful discussions. Research was partially funded by Fundación Antorchas and Conicet PID 3/3221/0092.

References

[1] L. Civale et al., Phys. Rev. Lett. 67 (1991) 648;
J. Thompson et al., Appl. Phys. Lett. 60 (1992) 2306;
M. Konczykowski et al., Phys. Rev. B 44 (1991) 7167;
W. Gerhauser et al., Phys. Rev. Lett. 68 (1992) 879;
R.C. Budhani et al., Phys Rev. Lett. 69 (1992) 3816.

[2] D.R. Nelson and V.M. Vinokur, Phys. Rev. B 48 (1993) 13060.

[3] G. Blatter, M.V. Feigel'man, V.B. Geshkenbein and V.M. Vinokur, Rev. Mod. Phys. 66 (1994) 1125.

[4] L. Krusin-Elbaum, L. Civale, G. Blatter, A. Marwick F. Holtzberg and C. Feild, Phys. Rev. Lett. 72 (1994) 1914.

[5] L. Krusin-Elbaum, L. Civale, J.R. Thompson and C. Field, Phys. Rev. B 53 (1996) 11744.

[6] W. Jiang, N.-C. Yeh, D.S. Reed, U. Kriplani, A.D. Beam, M. Konczykowski, T.A. Tombrello and F. Holtzberg, Phys. Rev. Lett. 72 (1994) 550.

[7] See, e.g., Magnetic Susceptibility of Superconductors and Other Spin Systems, eds. R.A. Hein, T.L. Francavilla and D.H. Liebenberg (Plenum, New York, 1992) and references therein.

[8] M. Konczykowski, Y. Wolfus, Y. Yeshurun and F. Holtzberg, Physica A 200 (1993) 305.

[9] C.J. van der Beek, M. Konczykowski, V.M. Vinokur, T.W. Li, P.H. Kes and G.W. Crabtree, Phys. Rev. Lett. 74 (1995) 1214.

[10] Y. Ando, H. Kubota, Y. Sato and I. Terasaki, Phys. Rev. B 50 (1994) 9680.

[11] D.S. Reed, N.-C. Yeh, W. Jiang, U. Kriplani, A.D. Beam and F. Holtzberg, Phys. Rev. B 49 (1994) 4384.

[12] M.W. Coffey and J.R. Clem, Phys. Rev. B 45 (1992) 9872.

[13] E.H. Brandt, Physica C 195 (1992) 1.

[14] A.E. Koshelev and V.M. Vinokur, Physica C 173 (1991) 465.

[15] C.J. van der Beek, V.B. Geshkenbein and V.M. Vinokur, Phys. Rev. B 48 (1993) 3393.

[16] L. Civale, in Ref. [7].

[17] L. Krusin-Elbaum, G. Blatter and L. Civale, Phys. Rev. Lett. 75 (1995) 187;
G. Blatter, unpublished.

[18] E.H. Brandt, Phys. Rev. B 49 (1994) 9024; ibid., B 50 (1994) 4034; B 50 (1994) 13833.

[19] J.R. Clem and A. Sanchez, Phys. Rev. B 50 (1994) 9355.

[20] A.M. Campbell, J. Phys. C 4 (1971) 3186;
A.M. Campbell and J.E. Evetts, Adv. Phys. 21 (1972) 199.

[21] F. de la Cruz, D. López and G. Nieva, Philos. Mag. B 70 (1994) 773.

[22] L. Civale, G. Pasquini, P. Levy, G. Nieva, D. Casa and H. Lanza, Physica C 263 (1996) 389.